Journal of Microwaves, Optoelectronics and Electromagnetic Applications, Vol. 20, No. 2, June 2021
DOI: http://dx.doi.org/10.1590/2179-10742021v20i21067

YIG Matrix Based Multiband Magneto-Dielectric Cylindrical Resonator Antenna

Andrécia Pereira da Costa[1], Glauco Fontgalland[1], Alfrêdo Gomes Neto[2], Antônio Sérgio B. Sombra[3]
[1]*Electrical Engineering Department, Federal University of Campina Grande, UFCG, Av. Aprígio Veloso, 882, Bldg. CJ, Universitário, CEP: 58.429-970, Campina Grande, Paraiba, Brazil, andrecia.costa@ee.ufcg.edu.br, fontgalland@dee.ufcg.edu.br*
[2]*Federal Institute of Education of Paraíba, IFPB, Av. 1st May, 720, João Pessoa, Paraíba, 58015-430, Brazil, alfredogomesjpa@gmail.com*
[3]*Department of Physics, Federal University of Ceará, UFC, Pici, Bldg. 930, 60020-181, Fortaleza, Ceará, Brazil, asbsombra@gmail.com*

***Abstract*— A multiband magneto-dielectric resonator antenna with cylindrical geometry is proposed in this paper. The resonator is composed of yttrium iron garnet (YIG) with chemical composition $Y_3Fe_2(FeO_4)_3$. The final structure is built on a low-cost FR4 dielectric substrate. With only one resonator, the antenna is able to resonate in three distinct controlled frequency bands. These are the three propagation modes $HEM_{11\delta}$, $TE_{01\delta}$, and $TM_{01\delta}$, which are possible to be independently controlled at each input port of the resonator antenna. The resonator's port was suitable designed to feed specific modes of the antenna using microstrip lines placed judiciously to excite each mode. Analytic, numerical, and experimental studies were performed and, after optimization, the final antenna design was obtained. The obtained simulated and measured S-parameters results are below -10 dB at the resonance frequencies 5.75 GHz, 6.86 GHz, and 8.37 GHz. The corresponding measured bandwidths are 370 MHz, 120 MHz, and 1060 MHz, respectively. The antenna has a total size of 32.5 × 32.5 × 8.35 mm³. Measured radiation patterns and gain are also presented and show good agreement when compared to simulated results.**

***Index Terms*—** magneto-dielectric material, multiports, resonator antenna, YIG.

I. INTRODUCTION

The dielectric resonator antennas (DRAs) have been investigated by several researchers in recent years, due to their attractive advantages, such as high dielectric constant (fundamental for the reduction of the size of the antennas), low metallic losses, broadband width, excitation facility, among others, has been incorporated to allow greater quality in the communication systems [1]-[5].

The antennas are manufactured with dielectric materials with low losses and high dielectric constant (ε_r) in the microwaves band. These materials are generally made of ceramic and can be produced in different geometries and sizes. [6], [7]. The most common geometries found in the literature are cylindrical, rectangular, half circle, and hemispherical. Among these geometries, the cylindrical shape offers greater configurational flexibility where the ratio between radius and height controls the resonance frequency (f_0) and the quality factor (Q) [3].

Brazilian Microwave and Optoelectronics Society-SBMO *received 28 Sept 2020; for review 28 Oct 2020; accepted 8 Apr 2021*
Brazilian Society of Electromagnetism-SBMag

ISSN 2179-1074

The dielectric resonators (DRs) have been used extensively for shielding in microwave circuits such as oscillators and filters [8]-[11]. It is also reported that the DRs mounted on top of ground planes or dielectric substrates can behave as radiators [12]-[16].

The paper in [17], made a study on the critical coupling resonator (CCR), in which a graphene-based hyperbolic metamaterial was proposed to replace the absorbing thin film in the critically coupled resonance. It is observed that the critical coupling frequency can be tuned by changing the thickness of the dielectric or the layer number of the graphene sheets in the unit cell of the graphene-dielectric (HMM). Another interesting work was addressed by [18] they demonstrated a thermally-controlled chiral switching in a hybrid metamaterial in the range of 1.4 THz. Vanadium dioxide film metal (VO2) was used, incorporated in two E-shaped resonators twisted by 90°, which allowed a dynamic control on polarization rotation angle, circular dichroism, and asymmetric transmission of linearly polarized light under external thermal excitation. A flexible polarization modulation in the THz frequency was also obtained, which would be important for applications such as thermal switching and polarization sensitive detection.

A new antennas' concept arises from DRAs based on the synthesis of different materials. They are the magneto-dielectric resonator antennas (MDRAs), which are found in the literature arising from ferrites. It is employed the magneto-dielectric material with high values of dielectric constant and magnetic constant (ε and μ) [19].

Ferrites are magnetic ceramic materials made up of a mixture of metallic and bivalent oxides, with iron oxide being the main component. They have physical properties such as high magnetic permeability, low dielectric losses, and elevated resistivity, making them attractive for applications in electronic devices that operate in microwave range [19]. According to their crystalline structures, the ferrites are classified into four groups: spinel, magnetoplumbite, garnet, and perovskite [19]. The garnet has lowest dielectric losses, therefore, suitable for many applications [20]. The yttrium iron garnet (YIG) is a special synthetic garnet with chemical composition $Y_3Fe_2(F_eO_4)_3$ [3], in which it was used by [21], in a double band MDCRA, it has two feed ports allowing independent control of two modes.

In this paper, it is presented a cylindrical multiband MDRA based on the magneto-dielectric resonator (MDR), which is composed of YIG ceramic matrix and a low-cost dielectric substrate FR4. The antenna's feeding access is composed of three microstrip line ports, allowing the simultaneously excitation of the three first modes $HEM_{11\delta}$, $TE_{01\delta}$, and $TM_{01\delta}$. Our design also provides the resonance of these three modes at frequencies 5.75 GHz, 6.86 GHz, and 8.37 GHz in a single resonator be independently controlled.

II. Materials and Methods

In this section it is presented the methodology to design a magneto-dielectric resonator antenna, with cylindrical geometry (MDCRA), presenting multiband frequency response. The proposed

Brazilian Microwave and Optoelectronics Society-SBMO *received 28 Sept 2020; for review 28 Oct 2020; accepted 8 Apr 2021*
Brazilian Society of Electromagnetism-SBMag *ISSN 2179-1074*

configuration is shown in Fig. 1. The MDCRA isometric view is shown in Fig. 1(a), while the top view of the feed mechanism is given in Fig. 1(b). Fig. 1(c) shows, the upper view with details of the central location of the MDR. The parameters with their respective dimensions of the proposed MDCRA are given in Table I.

The MDR has the following characteristics: $\varepsilon_{r,MDCRA} = 11.32$, $\mu_r = 1.10$, dielectric loss tangent $tan\delta_E = 0.00014$, magneto loss tangent $tan\delta_M = 0.00025$; with dimensions $D = 14.36mm$, $H = 6.85mm$. The FR4 fiberglass substrate used has thickness $H_s = 1.5mm$, dielectric constant $\varepsilon_{r,FR4} = 4.4$, and $tang_E = 0.019$. Fig. 2 shows the prototype of the proposed MDCRA manufactured. Isometric view, top view, and bottom view are shown in Figs. 2(a), 2(b), and 2(c), respectively.

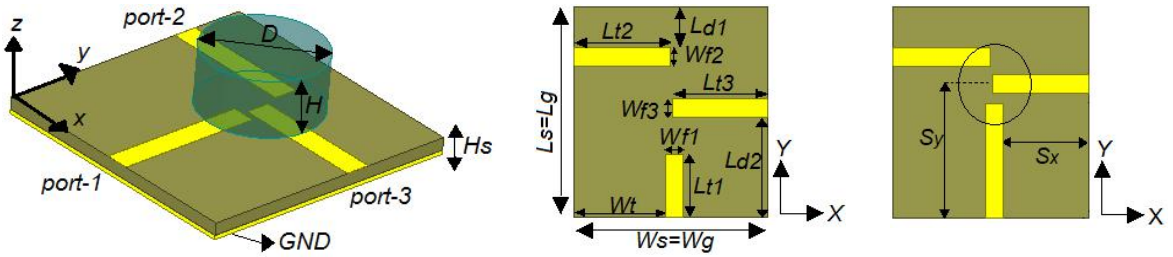

(a) (b) (c)

Fig. 1. Basic structure of the proposed MDCRA, (a) isometric view, (b) top view of the feed mechanism, and (c) upper view with detail location of the DR.

TABLE I. DESIGNED ANTENNA DIMENSIONS

	Substrates			Ground Plane			MDR			
Parameter	***Ls***	***Ws***	***Hs***	***L_g***	***W_g***	***GND***	***D***	***H***	***S_y***	***S_x***
Values (mm)	32.50	32.50	1.5	32.50	32.50	0.035	14.36	6.85	19.75	14.81

	Microstrip Line								
Parameter	***L_{t1}***	***L_{t2}***	***L_{t3}***	***L_{d1}***	***L_{d2}***	***W_t***	***W_{f1}***	***W_{f2}***	***W_{f3}***
Values (mm)	17.10	16.75	16.45	6.78	18.26	14.81	2.88	2.93	2.99

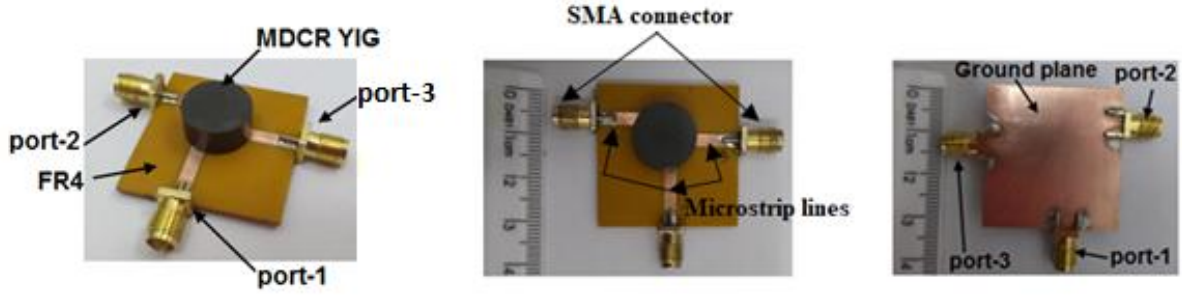

(a) (b) (c)

Fig. 2. Prototype of the proposed MDCRA, (a) Isometric view, (b) top view and (c) bottom view.

ISSN 2179-1074

III. EXCITATION METHOD OF $HEM_{11\delta}$, $TE_{01\delta}$ E $TM_{01\delta}$ MODES

The mathematical expression used for determine the resonance frequencies at each mode can be found at Equations 1, 4, and 5 in references [22]-[24]. It is possible to identify the frequencies 5.46 GHz, 7.40 GHz, and 8.53 GHz for the respective $HEM_{11\delta}$, $TE_{01\delta}$, and $TM_{01\delta}$ modes using the dimensions presented in Table I. The parameters W_{f1} and L_{t1} of the microstrip lines, highlighted in Table I, were necessary to produce the $HEM_{11\delta}$ mode at port 1.

For the microstrip feeding port 1, was first made a parametric study on the microstrip width W_{f1}, to determine the best adaptation to the impedance value of the 50 Ω input port 1. After that, the exact value of the length L_{t1} is obtained by determining the length that provides the first resonance frequency at 5.75 GHz. The same optimization tool box is used to reach the length of 1.71 cm. This frequency is close to the 5.46 GHz value obtained using Equation (1), used in [22].

$$f_{rHEM_{11\delta}} = \frac{6.321c}{2\pi r\sqrt{\varepsilon_{r_{eff}}+2}} \times \left[0.27 + 0.36\left(\frac{r}{2h_{eff}}\right) + 0.02\left(\frac{r}{2h_{eff}}\right)^2\right] \quad (1)$$

In which, $\varepsilon_{r_{eff}}$ is the effective dielectric constant and r is the radius of MDCRA, h_{eff} is the total height of proposed MDCRA design, and c is the speed of light. The value of $\varepsilon_{r,eff}$ and h_{eff} are determined by Equation (2) and Equation (3)

$$\varepsilon_{r_{eff}} = \frac{h_{eff}}{\frac{h}{\varepsilon_{r_{CDRA}}} + \frac{h_s}{\varepsilon_{r_{sub}}}} \quad (2)$$

and

$$h_{eff} = h + h_S. \quad (3)$$

The same principle was adopted for the feeding microstrip of port 2 and port 3, having width *Wf2* and *Wf3* and length *Lt2* and *Lt3*, respectively. These parameters allow to obtain the second resonance frequency at 6.85 GHz for the $TE_{01\delta}$ mode, which approaches the 7.40 GHz calculated using Equation (4) used in [23]. While the third resonance frequency at 8.39 GHz corresponding to the $TM_{01\delta}$ mode approaches to the value 8.53 GHz obtained using Equation (5), also applied in [22]

$$f_{rTE_{01\delta}} = \frac{c\sqrt{2.404 + \left(\frac{\pi r}{2h_{eff}}\right)^2}}{2\pi r\sqrt{\varepsilon_{r_{eff}}+2}} \quad (4)$$

and

$$f_{rTM_{01\delta}} = \frac{c\sqrt{3.831 + \left(\frac{\pi r}{2h_{eff}}\right)^2}}{2\pi r\sqrt{\varepsilon_{r_{eff}}+2}}. \quad (5)$$

Based on the fact that the resonance frequency is affected by the displacement of the MDR over the feeding ports the optimized position for MDR are S_y and S_x, the values are highlighted in Table I.

Brazilian Microwave and Optoelectronics Society-SBMO *received 28 Sept 2020; for review 28 Oct 2020; accepted 8 Apr 2021*
Brazilian Society of Electromagnetism-SBMag *ISSN 2179-1074*

IV. Simulated and Measured Results

The computer simulations were carried out in order to analyse the functionality of the resonant behaviour, isolation between the feeding microstrip, and the gain of the proposed MDCRA.

The studied antenna was designed and simulated using CST's Microwave studio, a computational program based on Finite Integration in Technique [25]. The proposed MDCRA antenna is fed by three planar strip lines producing three distinct resonance frequencies, with the possibility not only to excite three modes at the same time but also to excite each port independently at the same time or not.

The S-parameters measurements were carried on an anechoic chamber in the Metrology Laboratory (LABMET) of the UFCG, where a vector network analyser model ZVB 20, Rohde & Schwarz (10 to 20 GHz) and a reference antenna (log-periodic, model 106971, 1 GHz-10 GHz) were used at the receiver. The anechoic chamber used during the experiments is a compact SAVER ETS-R&S system ranging from 1 GHz to 18 GHz, model number S81 3x7 and serial number 1156. The system has a turntable facility and uses the EM32 system. The chamber has dimensions 7.3 x 3.2 x 4.1 m³ and magnetic tiles are placed on the floor to access its interior.

The results for the reflection and transmission coefficients, simulated and measured, for the MDCRA are displayed in the frequency range from 4.5 GHz to 9.5 GHz. The bandwidth is taken for the reflection coefficient S_{11} less than -10 dB. Fig. 3 gives a comparison of the three resonance frequencies where the first simulated resonance frequency was 5.75 GHz, which is in perfect agreement with the measured frequency at 5.75 GHz. The simulated and measured bandwidths were 300 MHz and 270 MHz, respectively. For the second resonance, the simulated and measured results were both 6.86 GHz, depicting a good agreement between the two results. Both simulated and measured bandwidths are 170 MHz. Finally, the third simulated resonance was 8.43 GHz, which is in agreement with the measured frequency of 8.37 GHz. The simulated and measured bandwidths are 1036 MHz and 1000 MHz, respectively. These results for the third resonance represent a difference of only 0.7 % in frequency and 3.5 % in BW. Analytically, the resonance frequencies calculated in the previous section, according to the equations highlighted in [17], show values close to the simulated and measured frequencies.

The isolation between the three feeding ports were evaluated through simulation and measurement, too. The simulation and measurements results for each individual port are presented in Figs.4, 5, and 6. The coupling between ports 1 and 2 is assessed measuring the transmission coefficient S_{21} and S_{12}. These results are given in Fig. 4, where it is possible to observe good isolation (S_{21}<-10dB) in the entire frequency range of the proposed MDCRA design. In Fig. 5, one can observe that the simulated and measured results for S_{13} and S_{31} are below -10 dB in the entire range from 4.5 GHz to 9.5 GHz. Moreover, within the mode 1 band and mode 2 band the isolation is -15 dB, except in the upper band of mode 3 that it reaches -12 dB.

received 28 Sept 2020; for review 28 Oct 2020; accepted 8 Apr 2021

ISSN 2179-1074

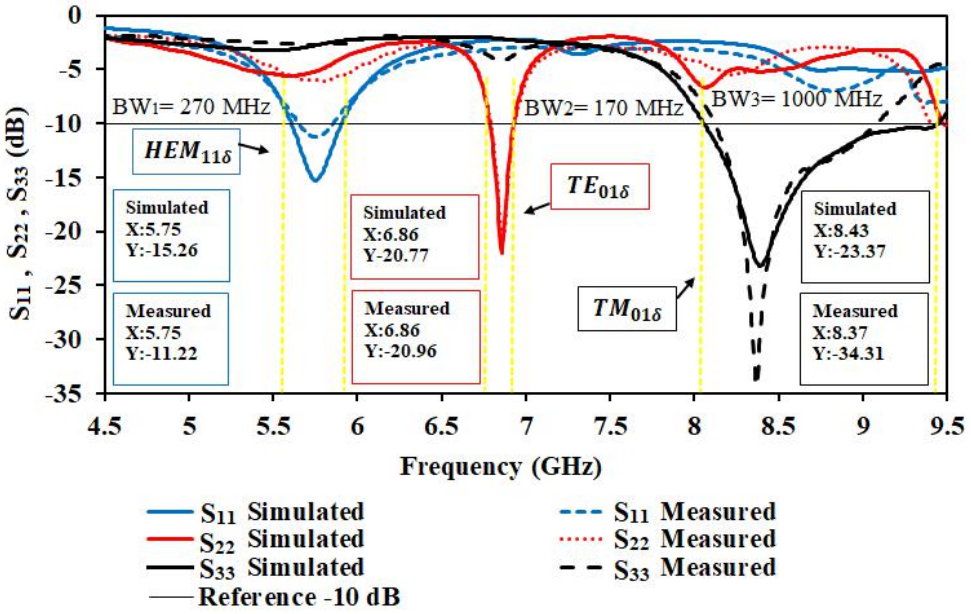

Fig. 3. S_{11}, S_{22} and S_{33} parameters simulated and measured for the proposed MDCRA.

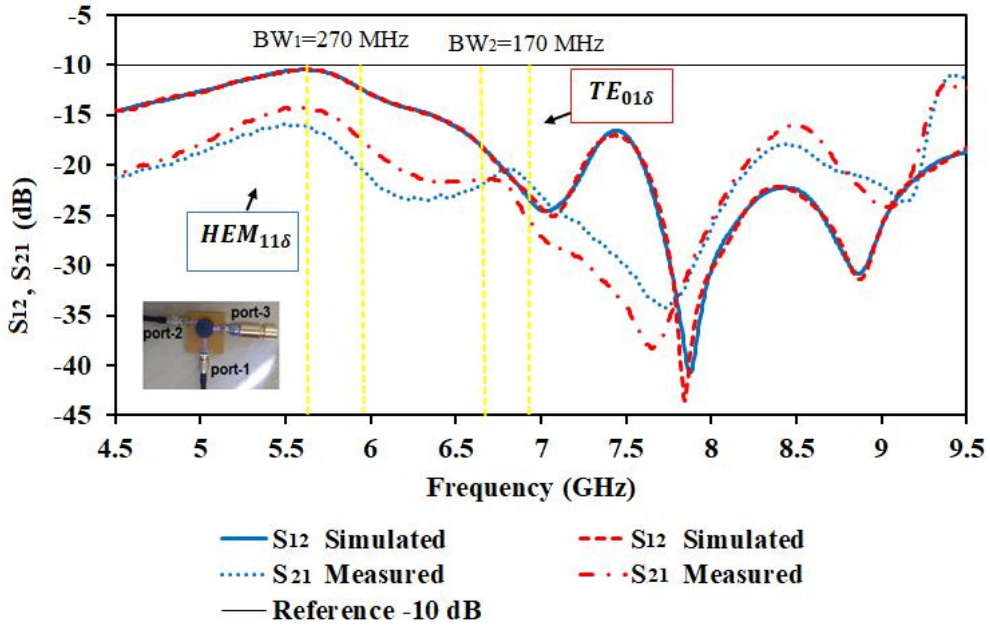

Fig. 4. S_{12}, S_{21} parameters simulated and measured for the proposed MDCRA.

ISSN 2179-1074

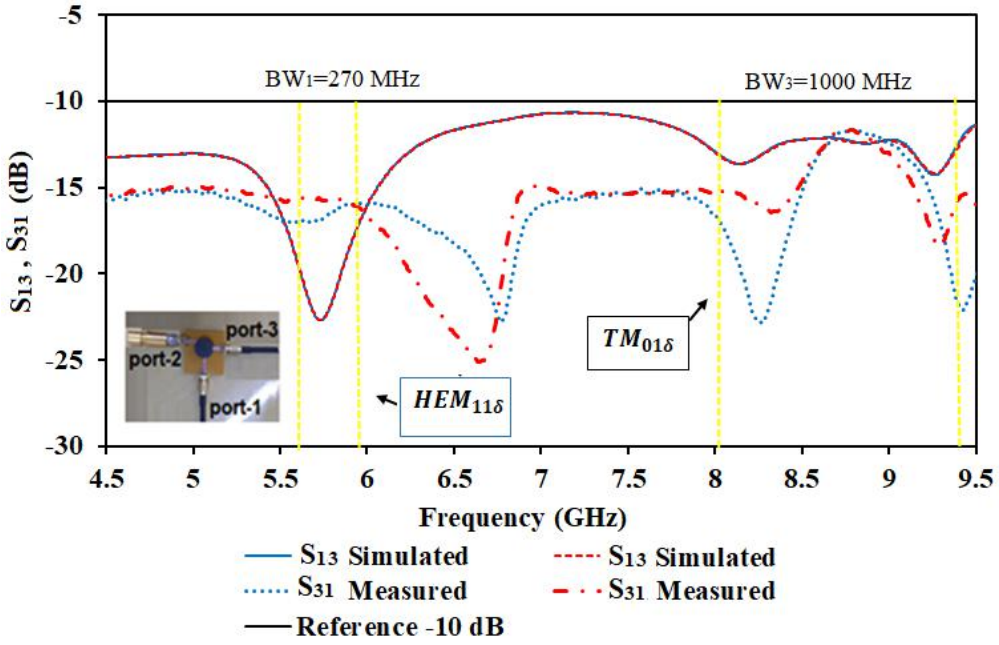

Fig. 5. S_{13}, S_{31} parameters simulated and measured for the proposed MDCRA.

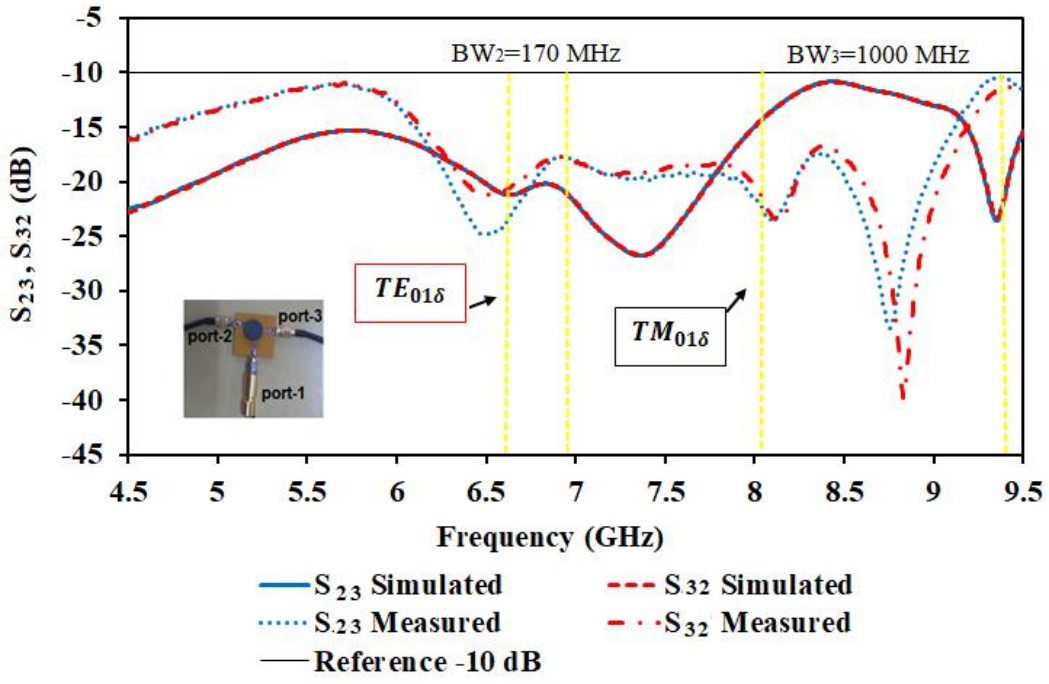

Fig. 6. S_{23}, S_{32} parameters simulated and measured for the proposed MDCRA.

ISSN 2179-1074

Fig. 6 highlights the simulated and measured results for the isolation between port 2 and 3 (S_{23} and S_{32}). It can be observed, that the isolation is below -10 dB in the entire simulated and measured band. A good agreement is also observed between the simulated and the measured results. For this case, the isolation between ports 2 and 3 are even better where within their bands the isolation is low as -18 dB. A comparison between the analytical, simulated, and measured results for the proposed MDCRA generating $HEM_{11\delta}$, $TE_{01\delta}$ and $TM_{01\delta}$ modes is highlighted in Table II.

Fig. 7 shows the simulated and measured far-field radiation pattern for the proposed MDCRA. The measurements were conducted inside an anechoic chamber at the LABMET – UFCG. The insertion losses in cables and connectors were disregarded. Although, there is a loss between 0.5 dB to 1 dB per adapter. It is observed the presence of cable's connection and matching load size, which this imposes some limitations to achieve the best performance results. Same differences between measurements and simulation are due to the considerable physical size of the load and connectors.

The antenna is designed to radiate in the perpendicular direction to its ground plane. The far-field at 5.75 GHz, 6.86 GHz, and 8.37 GHz for the E-plane and H-plane are presented in Fig. 7. For the measurement on the E-plane, the MDCRA was positioned in the horizontal plane (see Fig. 7). While for measurement on the H-plane the MDCRA was positioned in the vertical plane, considering each feeding ports. The simulated and measured directive gain of the MDCRA in the three frequency bands is shown in Table II. This table also shows the bandwidth and the S_{11} calculated, simulated, and measured.

A comparison of the proposed MDCRA in this paper with other works discussed in the literature are presented in Table III. It can be observed that the published papers on this topic have antennas with complex structures, bulky volume, and do not have the ability to control independently the propagation modes for operation at three resonances frequency. It is also noted that the MDCRA presents interesting properties for applications in systems that need small-sized devices and can be used for frequency control into the bands, as demonstrated in the proposed MDCRA.

received 28 Sept 2020; for review 28 Oct 2020; accepted 8 Apr 2021

ISSN 2179-1074

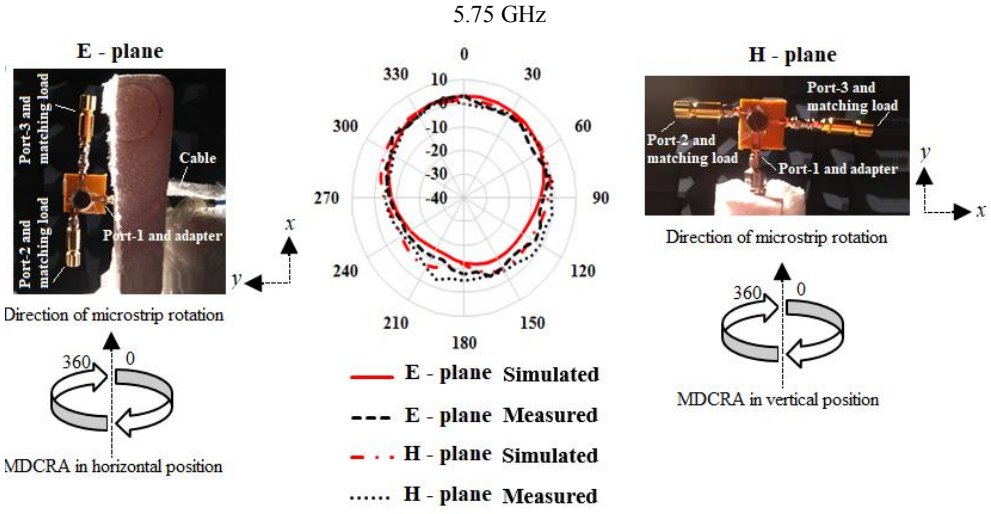

(a)

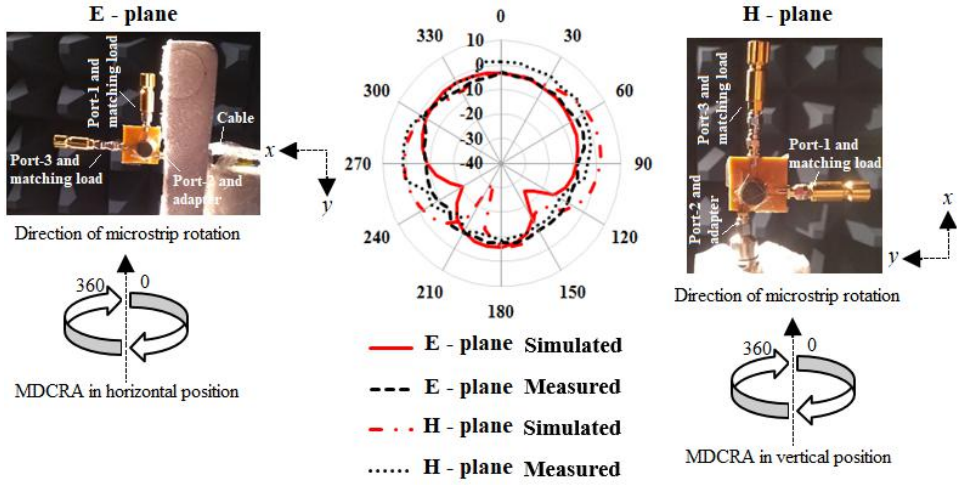

(b)

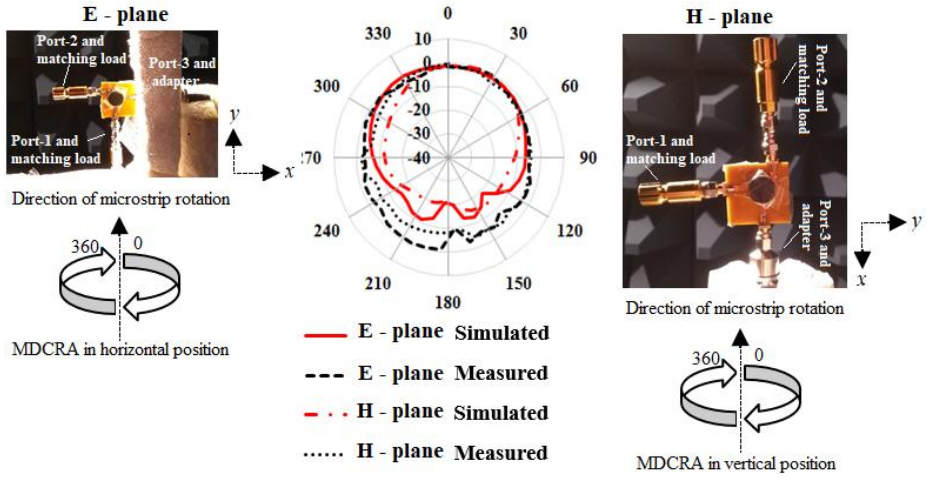

(c)

Fig. 7. Radiation pattern of proposed MDCRA at (a) 5.75 GHz, (b) 6.86 GHz and (c) 8.37 GHz.

ISSN 2179-1074

TABLE II. COMPARISON PARAMETERS PROPOSED MDCRA ANTENNA WITH THREE PORTS

Mode	Frequency (GHz)			Bandwidth (MHz)		S_{11} , S_{22}, S_{33} (dB)		Gain directive (dBi)	
	Analyt.	Simul.	Meas.	Simul.	Meas.	Simul.	Meas.	Simul.	Meas.
$HEM_{11\delta}$	5.46	5.75	5.75	300	270	-15.26	-11.22	3.54	2.6
$TE_{01\delta}$	7.4	6.86	6.86	170	170	-20.77	-20.96	2.65	1.85
$TM_{01\delta}$	8.53	8.43	8.37	1036	1000	-23.37	-34.31	2.74	1.95

TABLE III. COMPARISON OF THE PERFORMANCE OF THE PROPOSED MDCRA WITH OTHERS PUBLISHED IN THE LITERATURE

Parameters	Reference [26]	Reference [27]	Reference [28]	this work
Type of feed for excitation	Witched excitation probes	Microstrip lines and probe feed	Balanced-slots printed and Wilkinson power dividers printed	Microstrip lines
Antenna size, mm³	70 × 70 × 7.11	140 × 140 × 14.09	140 × 140 × 32.87	32.5 × 32.5 × 8.35
Resonator type	Hollow equilateral triangular dielectric resonator	Single elemento rectangular resonator	Single element cylindrical resonator	Single element cylindrical resonator
Number of feeding ports	Three	Three	Three	Three
f_0 (GHz) **measured**	5.7	8.76/9.3/10.2	2.4	5.75/6.86/8.37
$\varepsilon_r(tang)$	9.8	10.2	9.4	11.32
μ_r	1	1	1	1.10
Fabrication complexity	Complex	Complex	Moderate	Easy

V. CONCLUSIONS

In this paper, it is investigated a cylindrical MDCRA antenna with multiband characteristics, built from the MDR had using YIG composite, whose magnetic properties and the excitation method enabled the to generate the $HEM_{11\delta}$, $TE_{01\delta}$, and $TM_{01\delta}$ modes, which can be controlled individually on the same antenna. The proposed antenna exhibits operations in the 5.75 GHz, 6.86 GHz, and 8.37 GHz bands. A small difference between the simulated and measured results may have occurred due to the unconventional fabrication method used. It also exhibits good isolation between the ports within the investigated operation bands. Therefore, the cylindrical MDCRA has a small shape with multiband functionality, controllable frequencies, and modes. The results are satisfactory and shows strong potential for application in communication systems.

ACKNOWLEDGMENT

The authors thank the supported by the Coordination of the Post-Graduation Program in Electrical Engineering of the UFCG (COPELE) and Coordination for the Improvement of Higher Level Education Personnel (CAPES), the Group of Telecommunications and Applied Electromagnetism (GTEMA) the Federal Institute of Education, Science and Technology of Paraíba) and Physics Department of the Federal University of Ceará.

  ISSN 2179-1074

REFERENCES

[1] F. Wang, et al, "Ultra-wideband dielectric resonator antenna design based on multilayer form," *International Journal of Antennas and Propagation*, vol. 2019, Article ID 4391474, pp. 1-10, 2019.
[2] A. Gupta, R. K. Gangwar, "Hybrid rectangular dielectric resonator antenna for multiband applications", *IETE Technical Review,* vol. 37, no.1, pp. 83-90, 2019.
[3] K. M. Luk, and K. W. Leung, *Dielectric Resonator Antenas,* 1nd Edition, Baldock, Research Studies Press, 2003.
[4] M. Debab, Z. Mahdjoub, "Single Band Notched Characteristics UWB Antenna using a Cylindrical Dielectric Resonator and U-shaped Slot," *Journal of Microwaves, Optoelectronics and Electromagnetic Applications*, vol. 17, no. 3, pp. 340-351, 2018.
[5] P. W. S. Oliveira et al, "Experimental and numerical investigation of the microwave dielectric properties of the $MgTiO_3$ ceramic matrix added with $CaCu_3Ti_4O_{12}$," *Journal of Microwaves, Optoelectronics and Electromagnetic Applications*, vol. 16, no. 2, pp. 403-418, 2017.
[6] A. Petosa and A. Ittipiboon, "Dielectric resonator antennas: A historical review and the current state of the art," *IEEE Antennas and Propagation Magazine*, vol. 52, no.5, pp. 91-116, 2010.
[7] A. Sharma, P. Ranjan and R.K. Gangwar, "Multiband cylindrical dielectric resonator antenna for WLAN/WiMAX application," *IET Electronics Letter*, vol. 53, no. 3, pp. 132-134, 2017.
[8] M. S. Bakr, I. C. Hunter and W. Bösch, "Miniature Triple-Mode Dielectric Resonator Filters," *IEEE Transactions on Microwave Theory and Techniques*, vol. 66, no. 12, pp. 5625-5631, 2018.
[9] L. Zhou, J. Chen and Q. Xue, "Design of Compact Coaxial-Like Bandpass Filters Using Dielectric-Loaded Strip Resonator," *IEEE Transactions on Components, Packaging and Manufacturing Technology,* vol. 8, no. 3, pp. 456-464, 2018.
[10] J. Li, Y. Zhan, W. Qin, Y. Wu, and J. Chen, "Differential dielectric resonator filters," *IEEE Transactions. Components, Packaging and Manufacturing Technology,* vol. 7, no. 4, pp. 637-645, 2017.
[11] O. Kızılbey, O. Palamutçuoğulları and B. S. Yarman, "Design of low phase noise 7.7 GHz dielectric resonator oscillator," *2013 8th International Conference on Electrical and Electronics Engineering (ELECO)*, Bursa, Turkey, pp. 591-594, 2013.
[12] G. Varshney, V. S Pandey, R. S. Yaduvanshi, "Dual-band fan-blade-shaped circularly polarised dielectric resonator antenna," *Microwaves Antennas & Propagation IET*, vol. 11, no. 13, pp. 1868-1871, 2017.
[13] N. K. Mishra, S. Das and D. K. Vishwakarma, "Circularly polarized cylindrical dielectric resonator antenna for the X-band frequency," *2017 IEEE International Conference on Antenna Innovations & Modern Technologies for Ground, Aircraft and Satellite Applications (iAIM),* Bangalore, Índia, pp. 1-4, 2017.
[14] N. K. Mishra, S. Das and D. K. Vishwakarma, "Low-profile circularly polarized cylindrical dielectric resonator antenna coupled by L-shaped resonating slot," *Microwave and Optical Technology Letters*, vol. 59, no. 5, pp. 996-1000, 2017.
[15] G. Das, A. Sharma, R. K. Gangwar, and M. S. Sharawi, "Compact back-to-back DRA-based four-port MIMO antenna system with bi-directional diversity," *Electronics. Letters*, vol. 54, no. 14, pp. 884-886, 2018.
[16] J. E.V. de Morais, et al, "Magneto Tuning of a Ferrite Dielectric Resonator Antenna Based on $LiFe_5O_8$ Matrix, " *Journal of Electronic Materials*, vol. 47, no.7, pp. 3829-3835, 2018.
[17] Y. Xiang, X. Dai, J. Guo, et al. ''Critical coupling with graphene-based hyperbolic metamaterials." *Scientific Reports*, vol. 4, no. 5483, pp. 1-7, 2014.
[18] T.T. Lv, Y. X. Li, H. F. Ma, et al. ''Hybrid metamaterial switching for manipulating chirality based on VO_2 phase transition." *Scientific Reports, vol.* 6, no. 23186, pp.1-9, 2016.
[19] G. M. Picado. Characterization of $Y_3Fe_5O_{12}$ Prepared by Sintering and Microwave, University of Aveiro, Departamento of Physics, M.S. thesis, Aveiro, PT, 2012.
[20] P. B. A. Fechine, G. Fontgalland and A. S. B. Sombra, "New materials for miniaturized magneto-dielectric antennas based on $GdIG_xYIG_{1-x}$ composite," *2016 IEEE International Symposium on Antennas and Propagation (APSURSI)*, 2016, pp. 1939-1940.
[21] A. P. da Costa, G. Fontgalland, A. G. Neto, A. S. B. Sombra, R. R. M. do Valle, "Dual-frequency magneto-dielectric resonator antenna based in a YIG matrix with control of $HEM_{11\delta}$ and $TE_{01\delta}$ modes," *Microwave and Optical Technology Letters*, Early View, pp. 1-12, 2020.
[22] A. Sharma, G. Das, P. Ranjan, N. K. Sahu and R. K. Gangwar, "Novel feeding mechanism to stimulate triple radiating modes in cylindrical dielectric resonator antenna," *IEEE Access*, vol. 4, pp. 9987-9992, 2016.
[23] A. Petosa, *Dielectric Resonator Antenna Handbook*, 1nd Edition, Norwood, Artech House, 2007.
[24] D. Guha, P. Gupta and C. Kumar, "Dualband cylindrical dielectric resonator antenna employing $HEM_{11\delta}$ and $HEM_{12\delta}$ modes excited by new composite aperture," *IEEE Transactions on Antennas and Propagation*, vol. 63, no. 1, pp. 433-438, 2015.
[25] *CST Microwave Studio Suite*, version Student Edition, https://www.cst.com/. Accessed August 2019.
[26] A. Behloul, I. Messaoudene, T. A. Denidni and A. Benghalia, "Three-port triangular dielectric resonator antenna with switching beam forming operation", *Microwave and Optical Technology Letters*, vol. 59, no. 4, pp. 955-958, 2017.
[27] A. Abdalrazik, A. S. A. El-Hameed and A. B. Abdel-Rahman, "A Three-Port MIMO Dielectric Resonator Antenna Using Decoupled Modes," *IEEE Antennas and Wireless Propagation Letters*, vol. 16, pp. 3104-3107, 2017.
[28] X. S. Fang, K.W. Leung, and K. M. Luk, "Theory and Experiment of Three-Port Polarization-Diversity Cylindrical Dielectric Resonator Antenna," *IEEE Transactions on Antennas and Propagation,* vol. 62, no. 10, pp. 4945-4951, 2014.

received 28 Sept 2020; for review 28 Oct 2020; accepted 8 Apr 2021

ISSN 2179-1074